

Article

Active Compensation of Differential Group Delay in a Dual-Wavelength Pulsed Fiber Laser Driven by Quasi-Synchronous Pumping

Boris Nyushkov ^{1,2,*} , Aleksey Ivanenko ¹, Gleb Vishnyakov ¹, Alexey Kharauzov ³ and Sergey Smirnov ¹ ¹ Novosibirsk State University, 630090 Novosibirsk, Russia² Novosibirsk State Technical University, 630073 Novosibirsk, Russia³ Pavlov Institute of Physiology, RAS, 199034 Saint Petersburg, Russia

* Correspondence: b.nyushkov@nsu.ru

Abstract: We report on synchronized dual-wavelength (1.07 μm and 1.24 μm) pulsed lasing driven by a quasi-synchronous primary pumping (at 0.98 μm) of an Yb-doped fiber laser, which incorporates also a P_2O_5 -doped fiber as an intracavity Raman converter. The original method developed for such lasing does not require saturable absorbers (or optical modulators) and dispersion management. We demonstrated that the mechanism of the quasi-synchronous pumping enables the aforesaid stationary lasing in spite of significant differential group delay (DGD) inevitably acquired by light pulses with such different wavelengths during an intracavity round trip due to large normal chromatic dispersion. This DGD can be actively compensated at every round trip by the forced “acceleration” of the pulses at 1.07 μm in the Yb-doped active fiber due to the overrated frequency of the quasi-synchronous pumping at 0.98 μm . This mechanism is related to the particular pulse amplification dynamics in a such gain-modulated active fiber. The demonstrated approach to synchronized dual-wavelength pulsed lasing in a single-cavity fiber laser features remarkable simplicity and reliability. Our proof-of-concept setup enabled the stable two-wavelength generation of regular trains of nanosecond pulses with energy up to 34 nJ at equal repetition rates.



Citation: Nyushkov, B.; Ivanenko, A.; Vishnyakov, G.; Kharauzov, A.; Smirnov, S. Active Compensation of Differential Group Delay in a Dual-Wavelength Pulsed Fiber Laser Driven by Quasi-Synchronous Pumping. *Photonics* **2023**, *10*, 42. <https://doi.org/10.3390/photonics10010042>

Received: 21 November 2022

Revised: 14 December 2022

Accepted: 28 December 2022

Published: 31 December 2022

Keywords: dual-wavelength lasing; pulsed fiber laser; stimulated emission; Raman scattering

1. Introduction

Generation of synchronized pulse trains at sufficiently different wavelengths by means of a single laser system is required for many tasks, including lidar measurements, mid-infrared difference frequency generation, coherent Raman spectroscopy, and pump-probe experiments. Such a demand drives continued research into efficient methods of dual-wavelength pulsed lasing, especially in fiber lasers that offer design flexibility and wide choice of photonic phenomena to be used.

A typical approach to dual-wavelength pulse generation in a rare-earth-doped fiber laser relies on passive mode locking along with spectral profiling of intracavity transmission function. This allows coexistence of two wavelength-shifted pulse trains owing to inhomogeneously broadened gain [1–3]. Such a laser with a single active fiber can provide only moderate spacing ($\ll 100$ nm) of the lasing wavelengths within the common gain band. The reported lasers of this type usually require careful intracavity polarization control for proper dual-wavelength pulsed lasing. Moreover, their intracavity dispersion causes differential group delay and repetition rate shift between wavelength-shifted pulse trains.

A more sophisticated approach relies on the use of two different rare-earth-doped active fibers in two coupled cavities with a common saturable absorber that allows pulsed lasing simultaneously at two very distant wavelengths, e.g., at 1.55 μm and 1.88 μm [4] or at 1.03 μm and 1.53 μm [5]. This approach allows equalization of pulse repetition rates by relative adjustment of coupled cavities lengths [5]. However, this approach features more



Copyright: © 2022 by the authors. Licensee MDPI, Basel, Switzerland. This article is an open access article distributed under the terms and conditions of the Creative Commons Attribution (CC BY) license (<https://creativecommons.org/licenses/by/4.0/>).

experimental complexity. Moreover, the wavelength choice is still limited to amplification bands of rare-earth-doped fibers.

Lasing at wavelengths beyond rare-earth amplification bands is achievable with Raman scattering. Relevant pulsed laser sources usually rely on synchronous pumping of an external Raman fiber resonator by pulses from a mode-locked rare-earth-doped fiber laser [6–8]. The largest difference between the pump and Stokes wavelengths can be achieved with a Raman resonator built of a P₂O₅-doped fiber which features the extended (up to 1330 cm⁻¹) Raman frequency shift [9,10]. Nevertheless, such laser sources require precise adjustment of the Raman resonator length to match the group delay of Raman pulses with the repetition rate of the pump pulses. In addition to experimental complexity, such laser sources have rather moderate overall energy efficiency because of the limited energy coupling between the pumping laser and the external Raman resonator.

There are also a few reports on the feasibility of the dual-wavelength pulsed lasing via stimulated emission from rare-earth ions and Raman scattering in single-cavity all-fiber lasers with artificial saturable absorbers [11–13]. However, the reported single-cavity lasers also feature a significant experimental complexity. They require precise compensation for differential group delay between bicolor pulses (e.g., by means of intracavity wavelength-division delay lines [11,12] or a graded-index multimode fiber [13]) in order to ensure repeatable and effective interaction of the pump and Stokes pulses in a common cavity. Intervals between lasing wavelengths in the reported single-cavity lasers were determined by a Raman frequency shift of just 440 cm⁻¹, typical of conventional glass fibers.

It is worth noting also that all the above approaches utilize saturable absorbers to trigger pulsed operation via passive mode locking (at least at one of the lasing wavelengths). It ensures relatively short (typically picosecond) pulse duration. At the same time, it complicates the laser design, reduces reliability, and energy capability. Proper operation of a saturable absorber is possible within quite limited ranges of pulse energies and peak powers. Some artificial saturable absorbers may require careful intracavity polarization control for proper operation.

In this work, we proposed and studied a novel method for synchronized dual-wavelength pulsed lasing in a single-cavity all-fiber laser without any saturable absorber and adjustable delay lines. The concept of the method stems from the features of laser pulse shaping in rare-earth fiber lasers with quasi-synchronous pumping which were discovered in our preceding works [14,15]. Herein, we applied quasi-synchronous pumping at 980 nm to our proof-of-concept single-cavity fiber laser with two gain media, namely an Yb-doped fiber and a P₂O₅-doped fiber, to induce synchronized dual-wavelength pulsed lasing at ~1.07 μm and ~1.24 μm (via stimulated emission in the Yb-doped fiber and Raman scattering in the P₂O₅-doped fiber). We showed that the quasi-synchronous pumping enables the aforesaid stationary lasing in spite of significant differential group delay (DGD) acquired by light pulses with different wavelengths during their intracavity round trip. This DGD can be actively compensated at every round trip by the forced “acceleration” of the pulses at 1.07 μm in the Yb-doped active fiber, provided that the frequency of quasi-synchronous pumping at 0.98 μm is overrated to a proper degree. The mechanism underlying such an “acceleration” can be understood from our preceding works [14,15] and an early theoretical prediction about possible increase of propagation velocity of a wave packet in an amplifying medium [16]. It was also discussed below as an inherent part of the new lasing method.

2. Proposed Method

The concept of synchronized dual-wavelength (~1.07 μm and 1.24 μm) pulsed lasing in a hybrid (Yb-based and Raman-based) single-cavity fiber laser with quasi-synchronous primary pumping (at 0.98 μm) is illustrated in Figure 1 and conditioned by Equation (1).

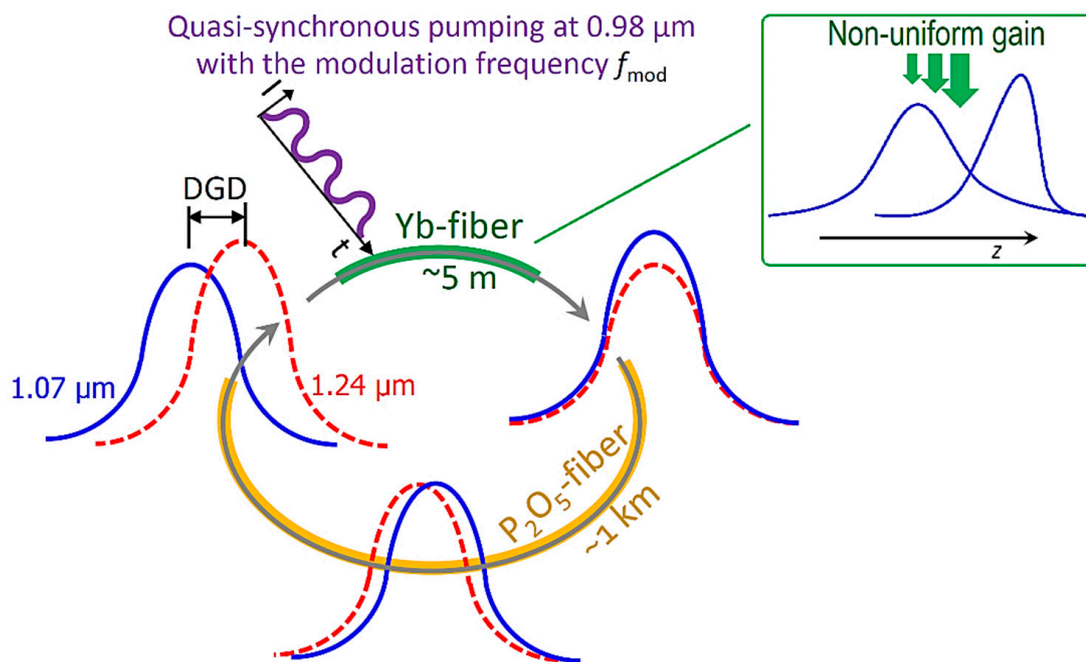


Figure 1. Concept of synchronized dual-wavelength ($\sim 1.07 \mu\text{m}$ and $1.24 \mu\text{m}$) pulsed lasing in a hybrid (Yb-based and Raman-based) single-cavity fiber laser with a quasi-synchronous primary pumping (at $0.98 \mu\text{m}$), which provides active compensation of differential group delay (DGD) between the fundamental ($1.07 \mu\text{m}$) and Stokes ($1.24 \mu\text{m}$) pulses. This DGD inevitably arises during intracavity round trip because of large normal chromatic dispersion introduced by a long Raman fiber. The compensation is achieved when completing the round trip with the forced “acceleration” of the retarded fundamental pulse in the Yb-doped active fiber, owing to the pumping-controlled non-uniform gain [14–16] as simplistically shown in the inset. Thus, the same superposition of the fundamental and Stokes pulses can be reproduced after every round trip, and therefore, the stationary synchronized dual-wavelength pulsed lasing becomes possible.

A simple fiber ring incorporates a relatively short (few meters) Yb-doped active fiber for lasing at $\sim 1.07 \mu\text{m}$ and a 1 km long P_2O_5 -doped Raman fiber for lasing at $\sim 1.24 \mu\text{m}$. Pulses generated at $1.07 \mu\text{m}$ play the role of pump pulses for the Raman fiber which provides the maximum gain for Stokes pulses at a frequency shift of about $1320\text{--}1330 \text{ cm}^{-1}$ [9]. The relatively large length of the Raman fiber ensures sufficiently high Raman gain in the laser. At the same time, owing to chromatic dispersion, such a long Raman fiber can cause significant DGD between pulses with different wavelengths. In particular, the DGD between pulses at $1.07 \mu\text{m}$ and $1.24 \mu\text{m}$ reaches 5.3 ns after their propagation in the 1 km long P_2O_5 -doped fiber. In accordance with the wavelength dependence of the effective refractive index of this fiber (Figure S1), the Stokes pulse ($1.24 \mu\text{m}$) propagates faster than the fundamental pulse ($1.07 \mu\text{m}$). This leads to a reduction of the effective interaction length for these pulses and limits the amplification of the Stokes pulse. In principle, this could be a serious impediment to stationary synchronized dual-wavelength pulsed lasing since such lasing requires repeatable (at every intracavity round trip) conditions for interactions of the fundamental and Stokes pulses. Nevertheless, in this work, we showed that the mechanism of the quasi-synchronous primary pumping at $0.98 \mu\text{m}$ enables such stationary lasing without any passive compensation for the intracavity DGD (e.g., without precisely adjusted wavelength-division delay lines, such as those used in [11,12]).

The quasi-synchronous modulation of the pump power at $0.98 \mu\text{m}$ above the lasing threshold of the Yb-based part of the proposed fiber laser can produce a regular train of nanosecond laser pulses at $\sim 1.07 \mu\text{m}$, which are much narrower than the pump modulation period. This happens due to gain non-uniformity experienced by the generated pulse, when

the pump power modulation frequency f_{mod} is slightly (by <1%) overrated as compared with the fundamental pulse repetition rate f_0 (determined by the free spectral range of the laser cavity in the vicinity of 1.07 μm). Such a pulse-shaping mechanism is described in detail in our preceding works [14,15]. Its following features are the principles for the proposed dual-wavelength lasing: (1) the fine tuning of the slightly overrated modulation frequency f_{mod} allows a gradual adjustment of duration and peak power of laser pulses at 1.07 μm ; (2) the fine tuning of the slightly overrated modulation frequency f_{mod} pulls accordingly the repetition rate of laser pulses at 1.07 μm ; (3) the slight mismatch between the modulation period ($1/f_{\text{mod}}$) and the intracavity group delay of a free-running laser pulse at 1.07 μm is compensated by its forced “acceleration” in the Yb-doped active fiber due to the stronger amplification of the leading pulse edge (see the inset in Figure 1).

Thus, when the quasi-synchronous primary pumping at 0.98 μm has shaped laser pulses at $\sim 1.07 \mu\text{m}$ with the instantaneous power remaining high enough during interaction time long enough to overcome the Raman lasing threshold, one may expect also occurrence of pulsed lasing at $\sim 1.24 \mu\text{m}$. However, the stationary lasing condition requires zeroing of the dispersion-induced DGD between the pulses at 1.07 μm and 1.24 μm after every intracavity round trip. The above-listed features of the quasi-synchronous pumping suggest that the proper overrating of the modulation frequency f_{mod} can provide active compensation of the DGD. Indeed, the Stokes (1.24 μm) pulses propagates faster than the pump (1.07 μm) pulses in the normal-dispersion P_2O_5 -doped fiber. At the same time, laser pulses at 1.07 μm experience a forced “acceleration” in the Yb-doped active fiber owing to the quasi-synchronous primary pumping at 0.98 μm . This “acceleration” is governed by the overrating of the modulation frequency f_{mod} as compared with the fundamental pulse repetition rate f_0 (determined by the free spectral range of the laser cavity in the vicinity of 1.07 μm). [14,15]. Therefore, it is possible to derive the relation between the DGD to be compensated and the properly overrated modulation frequency f_{mod} required for such a compensation:

$$DGD = \frac{1}{f_0} - \frac{m}{f_{\text{mod}}} \quad (1)$$

where m is an integer number. Herein, we explored the case of $m = 1$, while one can consider $m > 1$ for operation at the m -th harmonic of the fundamental pulse repetition rate.

3. Experimental Results and Discussions

As a proof of concept, we obtained and examined dual-wavelength pulsed lasing driven by a quasi-synchronous pumping in an experimental laser configuration shown in Figure 2. This configuration is based on an all-fiber ring cavity which includes two gain media, namely, an Yb-doped fiber for lasing at $\sim 1.07 \mu\text{m}$ and a P_2O_5 -doped Raman fiber for lasing at $\sim 1.24 \mu\text{m}$.

All fibers employed in the laser configuration were single-mode at the lasing wavelengths. The 1 km long P_2O_5 -doped fiber (FORC—Photonics PDF-5/125) provided Raman gains ($>5 \text{ dB/km}\cdot\text{W}$) at a frequency shift of about 1330 cm^{-1} . The 4.5 m long highly doped Yb-fiber (LIEKKI Yb1200-6/125DC) had a double-clad design. The intensity-modulated pump radiation at 0.98 μm from a fiber-coupled laser diode was injected into the inner cladding of the Yb-doped fiber via a fiber combiner. Unabsorbed residual pump radiation (if any) had no way to be efficiently coupled from the inner cladding of the Yb fiber to the core of the subsequent conventional single-clad fiber-optics elements. We examined the spectral purity of laser radiation acquired via a 5% coupler and found no residual pump radiation (as corroborated by Figure S2).

An 8 nm bandpass spectral filter centered at 1064 nm (according to its specification) was installed in the cavity for a rough selection of the desirable fundamental lasing wavelength. We had to use also a linked coupler of wavelength-division multiplexors (WDMs 1.07/1.24 μm) to form a bypass which allowed Raman radiation to avoid excessive intracavity losses (especially losses in the aforesaid bandpass spectral filter).

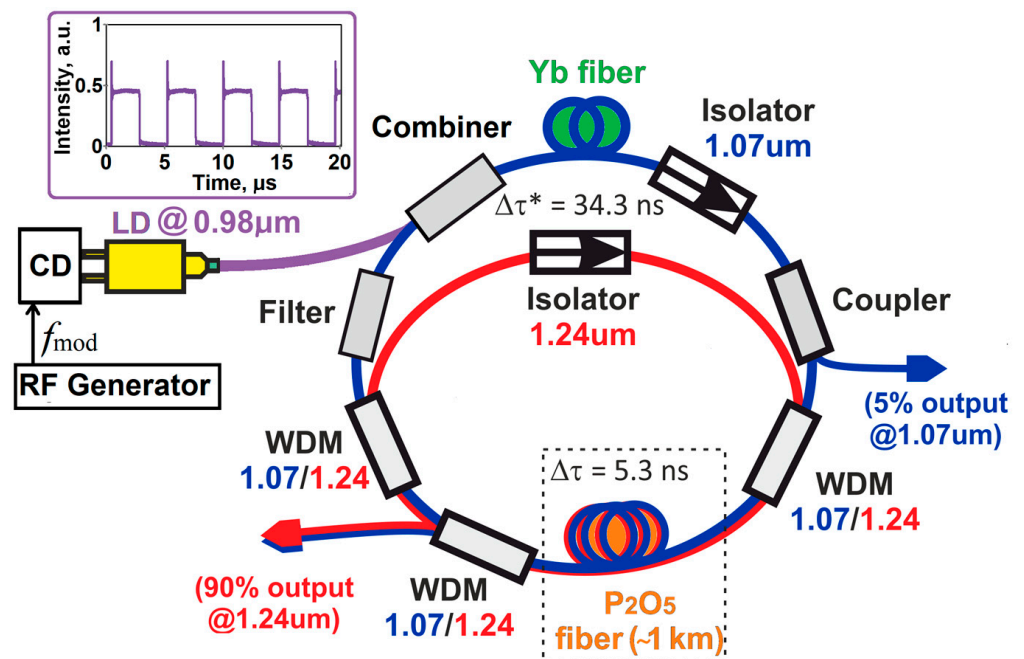


Figure 2. The proof-of-concept experimental laser configuration. LD—current-modulated laser diode for quasi-synchronous primary pumping at 0.98 μm; CD—current driver; WDMs—wavelength-division multiplexors; $\Delta\tau$ and $\Delta\tau^*$ designate contributions to the overall DGD from the P₂O₅-doped fiber and the intracavity bypass. The inset shows the measured time trace of the quasi-synchronously modulated pump power (pumping radiation was accessed via a 1% tap coupler, which is not shown in this scheme.).

It worth noting that the bypass did not serve for the compensation of the differential group delay between the generated bicolor pulses. On the contrary, it introduced an extra DGD with the same sign as the DGD acquired by the bicolor pulses in the common, 1 km-long, Raman fiber part of the cavity. The proposed concept does not require any length adjustment of separate optical paths for pulses with different wavelengths, unlike earlier dual-wavelength single-cavity laser systems [11,12].

The DGD acquired in the P₂O₅-doped Raman fiber was about 5.3 ns. In addition, Raman radiation completed the intracavity round trip via the fiber-optic bypass which was 7 m shorter than the fiber-optic pass of the fundamental radiation. This pass difference introduced an extra DGD of about 34.3 ns per round trip. Thus, the total DGD reached ~39.6 ns per round trip. Nevertheless, we have proven experimentally that the proposed method (relying on the quasi-synchronous pumping of the laser) enables active compensation of such a large DGD and, thus, allows stationary synchronized dual-wavelength pulsed lasing.

To provide a quasi-synchronous pumping, the laser diode current was digitally driven in a such way which led to a near-square-wave modulation of the pump power at 0.98 μm (see the inset in Figure 2). This form of modulation was unchangeable during experiments. A narrow overshoot appearing at the front of the pump pulses is typical for the step response of the bandlimited systems such as the pumping laser diode with its current driving circuit. Nevertheless, such overshoots could not seriously affect the laser gain dynamics in the Yb-doped active fiber because of the two reasons. First, they transferred a very low fraction of the overall pump energy (~1% per duty cycle). Second, the flat-top power level of the pumping pulses and their average power were both a few times higher than the lasing threshold. The current driver was clocked by an external tunable radiofrequency (RF) generator. This made possible the fine tuning of the pump power modulation frequency f_{mod} in the vicinity of the fundamental pulse repetition rate f_0

(determined by the free spectral range of the laser cavity near the lasing wavelength of 1.07 μm). In the examined laser configuration, this parameter amounted to about 207 kHz.

It is worth noting that without the pump power modulation, the continuous-wave (cw) lasing threshold at 1.07 μm was achieved with a relatively low (~ 0.2 W) pump power at 0.98 μm , while the achievement of the cw lasing threshold at 1.24 μm required a much higher (up to 4.5 W) pump power at 0.98 μm . This is not only due to the “cascaded” pumping of Raman-based lasing via the Yb-based lasing, but also due to significant difference in intracavity gain/loss properties at those lasing wavelengths. In particular, the WDM-1.07/1.24 installed right after the P₂O₅-doped fiber provided an approximately 90% output coupling for the Raman emission (in accordance with the provided wavelength channel isolation of 10 dB).

Nevertheless, we found that the proposed quasi-synchronous pumping allowed shaping of laser pulses at 1.07 μm with a peak power high enough to be well-above the Raman lasing threshold even when applying a moderate (≥ 1.5 W) average pump power at 0.98 μm . To set quasi-synchronous pumping properly for synchronized dual-wavelength pulsed lasing, we performed a sweep of the pump power modulation frequency f_{mod} around the fundamental pulse repetition rate ($f_0 \approx 207$ kHz) and simultaneously monitored laser radiation characteristics at both the fundamental (~ 1.07 μm) and Stokes (~ 1.24 μm) wavelengths. Below, we mainly report characteristics of such lasing at an average pump power of ~ 1.7 W. It should be noted, however, that such lasing is found to be reliably accessible and featuring similar characteristics at any average pump power in the range from ~ 1.5 to 2 W (as testified by the supplementary measurement results in Figures S3 and S4).

Figure 3 illustrates the evolutions of temporal and spectral characteristics of laser radiation at the above-indicated wavelengths which was measured upon the modulation frequency sweep in the vicinity of $f_0 \approx 207$ kHz. Downward approaching to this rate led to gradual evolution of lasing at the fundamental wavelength from barely modulated continuous-wave operation to shaping a regular train of high-contrast pulses. Figure 3a illustrates the corresponding evolution of temporal distribution of lasing power at ~ 1.07 μm , which was retrieved from serial oscilloscopic measurements. Shaping of high-contrast pulses was inherently accompanied with the rise of their peak power. At a certain instance, it became well-above the Raman lasing threshold, thereby leading to emergence of laser pulses at the Stokes wavelength (~ 1.24 μm) as seen in Figure 3b. Lasing at the Stokes wavelength appeared, only when the modulation frequency f_{mod} fell into the narrow range of approximately $207.5 \div 209$ kHz. Within this range, the quasi-synchronous pumping provided both the pulse shaping and the DGD compensation for the stationary dual-wavelength pulsed lasing. Figure 3c,d illustrate the corresponding spectral evolutions of lasing at the fundamental (~ 1.07 μm) and Stokes (~ 1.24 μm) wavelengths, respectively, as retrieved from serial measurements of optical spectra.

Measurements of the average power at each lasing wavelength conducted in conjunction with the modulation frequency sweep also corroborated the resonant emergence of Raman lasing when the modulation frequency fell into the range of $\sim 207.5 \div 209$ kHz as seen in Figure 4. The examined laser radiation was extracted through the WDM following the P₂O₅-doped fiber and purely separated by wavelength via external filtering. Figure 5 shows typical temporal and spectral traces acquired with the modulation frequency being alternatively set within and slightly beyond the aforesaid range. They revealed how the quasi-synchronous pumping at an overrated (relative to f_0) frequency triggers dual-wavelength pulsed lasing.

Further, we examined in detail the steady dual-wavelength pulsed operation at a modulation frequency of 208.8 kHz empirically selected from the above stated range providing the shortest pulse duration. Figure 6 represents the optical spectrum of laser radiation measured with a resolution of 0.1 nm in a wide span of 200 nm which captured both the fundamental (~ 1.07 μm) and Stokes (~ 1.24 μm) lasing wavelengths separated by the Raman frequency shift of about 1330 cm^{-1} , typical of P₂O₅-doped fibers. It is worth noting that the spectrum had no Stokes components with the Raman frequency shift of 440 cm^{-1} , typical

of conventional glass fibers. Such a Stokes component was suppressed by the specific wavelength selectivity of the WDMs and the bandpass filter in the laser cavity. Moreover, lasing at such a Stokes wavelength would require specific tuning of the modulation frequency to provide proper DGD compensation. The zooming of the optical spectrum in the vicinities of each lasing wavelength (insets in Figure 6) allows one to evaluate more precisely spectral widths and central (or peak) wavelengths for the generated bicolor pulses. They had close spectral widths of about 0.6 nm (at half maximum). Their peak wavelengths were evaluated to be about 1066.7 nm and about 1242.3 nm (with accuracy limited to the spectral resolution). The temporal characteristics of the obtained dual-wavelength lasing were examined by measuring simultaneously time traces of pulse trains at the fundamental and Stokes wavelengths as represented by oscillograms in Figures 7 and 8. In spite of a nearly equal spectral width, the generated bicolor pulses featured significant difference in their duration and shape. The Stokes pulses had a much shorter duration (43 ns) and a more regular shape as compared with the fundamental pulses. This was caused by mutually affected shaping of pulses at the fundamental and Stokes wavelengths in the Raman fiber. A more optimal compromise between pulse shortening, GDD compensation, and secondary pump depletion can be achieved in future to enable generation of bicolor pulses with comparable temporal envelopes. Nevertheless, the demonstrated strong shortening of the Stokes pulses (down to 43 ns) as compared with the modulation period ($\sim 4.8 \mu\text{s}$) of the primary pump power was already very remarkable achievement. It is worth noting also that adjustment of the average pump power at $0.98 \mu\text{m}$ within the allowable range of ~ 1.5 to 2 W caused a moderate change of the minimum achievable pulse duration. It was varied from $\sim 38 \text{ ns}$ to 51 ns , when we changed the average pump power from 1.55 to 1.9 W as shown in Figure S4.

According to the average output power characteristics shown in Figure 4, the pulse energies at both lasing wavelengths could reach nearly 34 nJ , when the pump modulation frequency (which determines the pulse repetition rate) was in the vicinity of 208 kHz . Actually, such an energy evaluation is just an upper estimate for the Stokes pulse and a lower estimate for the fundamental pulse, at the given average primary pump power.

Optionally, one can exploit the 5% output coupler following the Yb-doped fiber to access the fundamental radiation with a much higher average power (up to 7 times) as compared with that accessed via the WDM following the Raman fiber.

To demonstrate the stability of the achieved synchronous dual-wavelength pulsed lasing, we performed multiple oscilloscopic measurements (synchronously at each lasing wavelength) and acquired large series of the corresponding time traces for comparison. The time traces were acquired every minute during an hour as represented in Figure 8. As one can see, the pulse trains at the fundamental and Stokes wavelengths were rather stable and had the same pulse repetition period of about $4.8 \mu\text{s}$. They featured relatively high amplitude stability: the root-mean-square (RMS) noise was just about 3% in the worst case of the Stokes pulse train.

The radio-frequency (RF) spectra of the pulse trains at the fundamental and Stokes wavelengths were measured and compared as well. Figure 9a represents an overlay of their RF spectra measured across the same relatively wide frequency span. These spectra featured the equidistant discrete structure with the frequency spacing equal to the pulse repetition rate. Figure 9b manifests the exact frequency fit of additionally measured high-resolution RF spectra of the fundamental and Stokes pulse trains, thereby testifying to their synchronization (equality of their pulse repetition rates). The measured pulse repetition rates both equaled to the pump power modulation frequency ($f_{\text{mod}} = 208.8 \text{ kHz}$). This is in a full agreement with the proposed concept of the active compensation of the DGD.

It is worth noting also that experimental data (namely, the actual values of f_0 , f_{mod} , and DGD) fitted Equation (1) fairly well, thereby validating the proposed method.

In continuation of the discussion, we would like to outline prospects for the further development of the reported method.

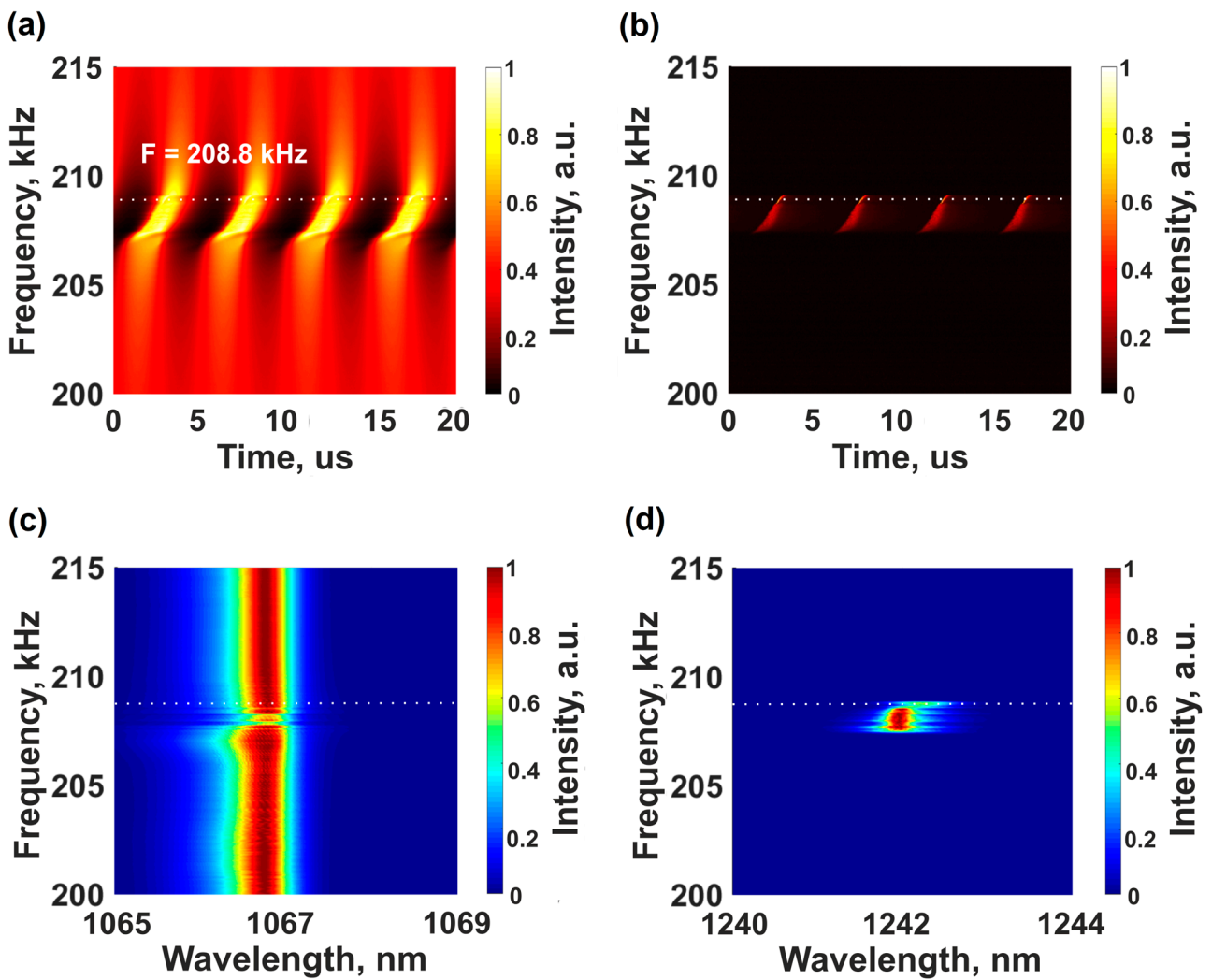


Figure 3. Evolution of temporal and spectral characteristics of laser radiation which was measured upon the modulation frequency sweep in the vicinity of the fundamental pulse repetition rate: (a) evolution of temporal distribution of lasing power at the fundamental wavelength ($\sim 1.07 \mu\text{m}$); (b) evolution of temporal distribution of lasing power at the Stokes wavelength ($\sim 1.24 \mu\text{m}$); (c) evolution of spectral distribution of lasing power at the fundamental wavelength ($\sim 1.07 \mu\text{m}$); (d) evolution of spectral distribution of lasing power at the Stokes wavelength ($\sim 1.24 \mu\text{m}$). The dotted white lines indicate the frequency ($F = 208.8 \text{ kHz}$) at which the dual-wavelength pulsed lasing was further examined.

Based on our previous studies [14,15], we believe that the quasi-synchronous pumping with the modulation frequency set close to a high harmonic of the fundamental pulse repetition rate will enable dual-wavelength pulsed lasing at a correspondingly high repetition rate. This possibility will be examined in our further research, which will be also aimed at obtaining shorter pulse durations.

In our previous study [15], we have shown also that the quasi-synchronous pumping of a single-wavelength Yb-fiber laser allows (in principle) obtaining a pulse duration as short as $\sim 10^{-3}$ of the pump modulation period. Thus, one can expect possible approaching to a pulse duration of the order of 1 ns upon the fine optimization of parameters of the proposed dual-wavelength laser configuration. Further pulse shortening will be energetically hampered by quick reduction of the overlap between the fundamental and Stokes pulses, as they propagate in the Raman fiber due to their group velocity mismatch (if the shortening is supposed to be similar for the both pulses) [17].

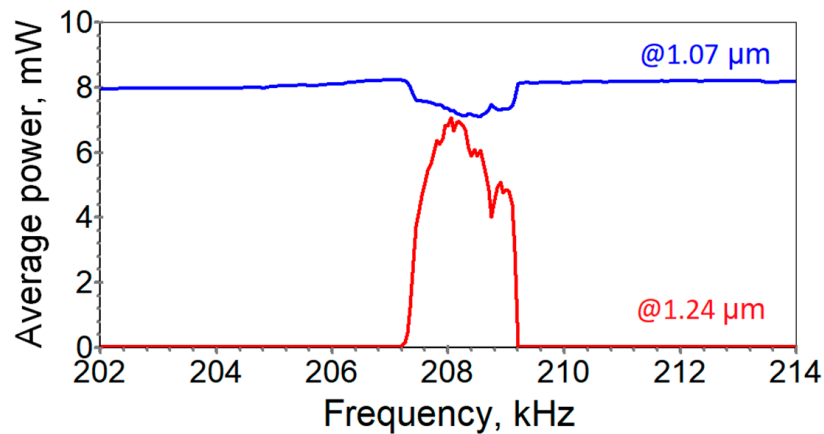


Figure 4. Dependence of the average output power at each lasing wavelength (1.07 μm and 1.24 μm) on the modulation frequency of the quasi-synchronous pumping.

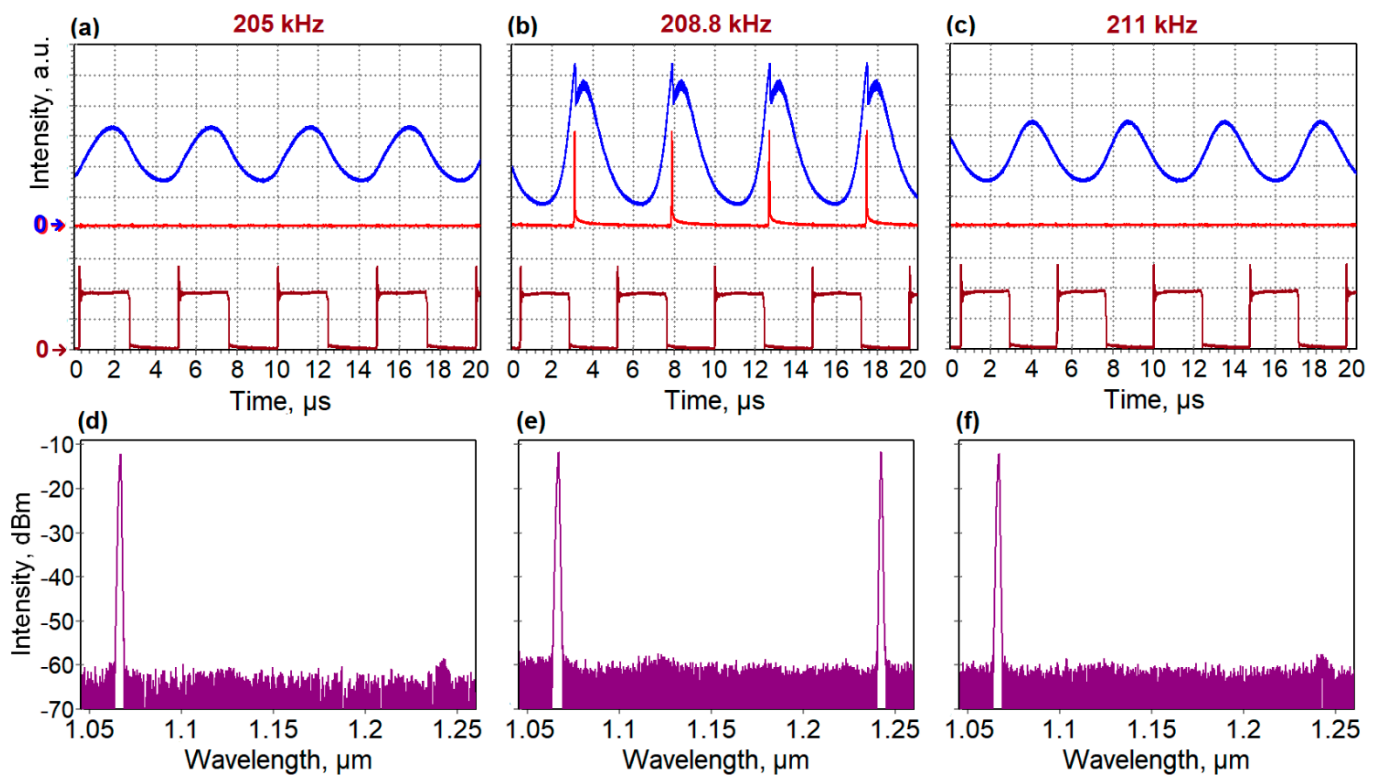


Figure 5. Temporal (a–c) and spectral (d–f) traces acquired at different modulation frequencies selected within and beyond the Raman power resonance shown in Figure 4. The legends of the oscillograms (a–c): blue traces—the fundamental radiation at 1.07 μm ; red traces—the Stokes radiation at 1.24 μm ; and brown traces—the pump radiation at 0.98 μm .

Of the practical interest may be also possible ways to adjust the power ratio of the fundamental and Stokes radiations. The difference in dependences of the fundamental and Stokes radiation powers on the modulation frequency (Figure 4) enabled a limited adjustment of the power ratio by fine tuning of the modulation frequency. The power ratio can be also controlled by varying the average pump power at 0.98 μm within the allowable range from ~ 1.5 to ~ 2 W. This allowed us to change noticeably the power ratio of the fundamental and Stokes radiations (roughly from 3:2 to 2:3) at the examined output as corroborated by the spectral power distributions in Figure S3d–f. When setting the average

pump power above 2 W, the dual-wavelength pulsed lasing became much noisier and less stable.

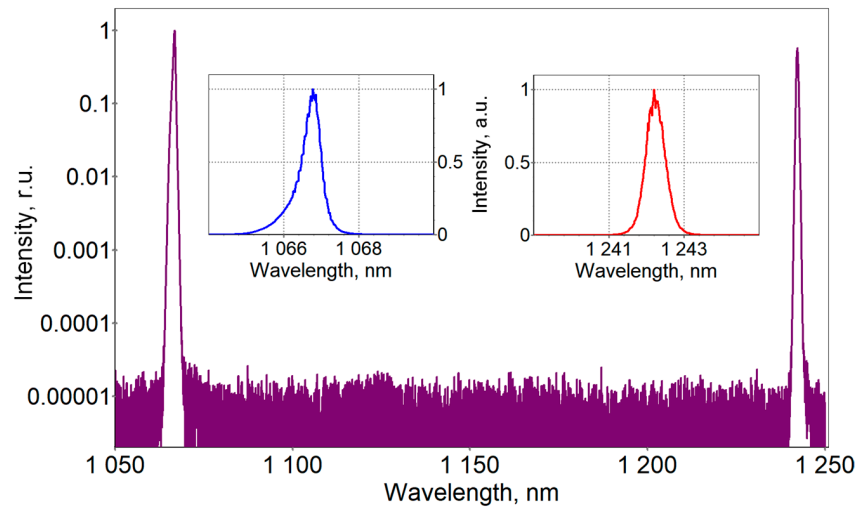


Figure 6. Measured optical spectrum of the dual-wavelength pulsed laser radiation obtained upon a quasi-synchronous pumping with the modulation frequency of 208.8 kHz (resolution: 0.1 nm). The spectrum was acquired via the WDM following the P₂O₅-doped fiber. Insets represent zooming in the vicinities of the fundamental (left) and Stokes (right) wavelengths.

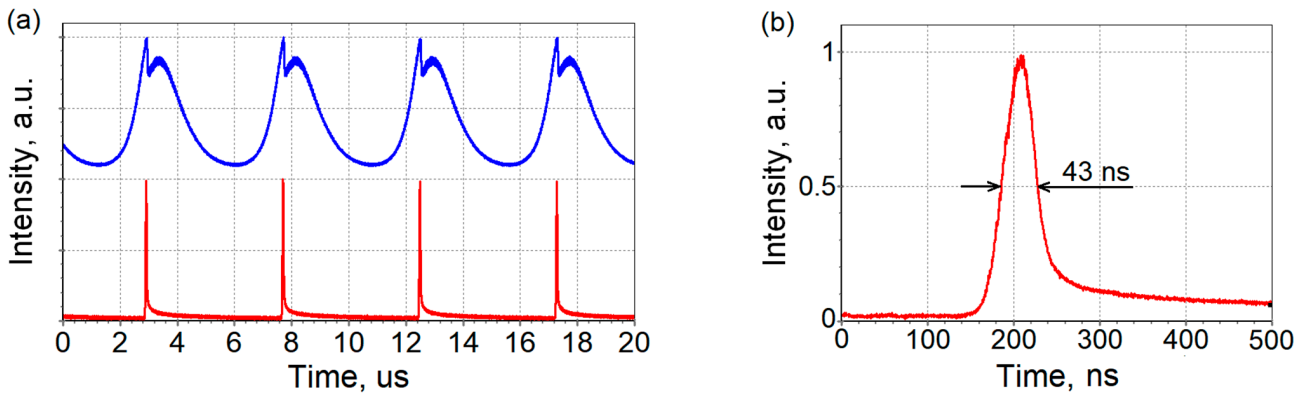


Figure 7. (a) Synchronously measured time traces of the laser pulse trains obtained at the fundamental (upper trace) and Stokes (lower trace) wavelengths upon a quasi-synchronous pumping with the modulation frequency of 208.8 kHz; (b) measured high-resolution time trace of a single laser pulse at the Stokes wavelength.

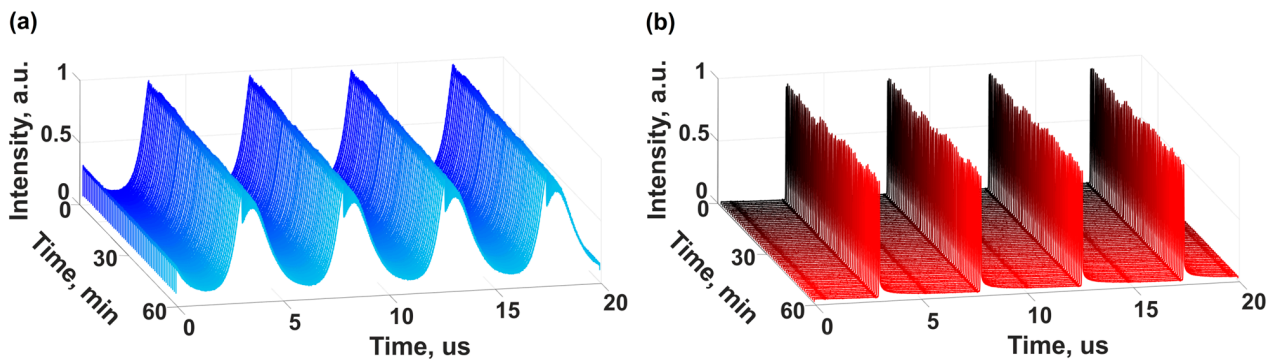


Figure 8. Series of time traces acquired with 1 min intervals during an hour for the pulse trains obtained at the fundamental (a) and Stokes (b) wavelengths upon a quasi-synchronous pumping with the modulation frequency of 208.8 kHz.

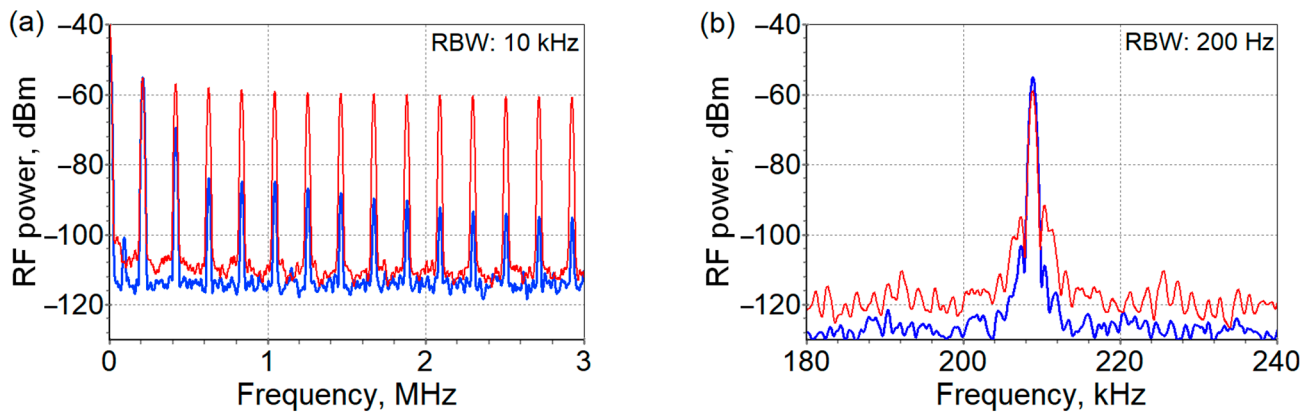


Figure 9. Overlay of the measured RF spectra of the fundamental (blue traces) and Stokes (red traces) pulse trains generated upon a quasi-synchronous pumping with the modulation frequency of 208.8 kHz. (a) Low-resolution RF spectra measured across a relatively wide frequency span; (b) high-resolution RF spectra measured in the vicinity of the modulation frequency. The RBW specifies the resolution bandwidth used to measure the RF spectra.

Finally, one might adjust and optimize the Raman fiber length and the optical feedback ratio provided for the Raman radiation. This is an efficient approach to static control of energy characteristics in the fiber lasers employing Raman gain, as it was shown, for example, in the works [12,18].

4. Conclusions

We have proposed a novel method for synchronized dual-wavelength pulsed lasing based on an actively controlled interplay of stimulated emission from rare-earth ions and Raman scattering in a shared all-fiber cavity. The method relies on the quasi-synchronous primary pumping and eliminates the need for saturable absorbers (or optical modulators) and adjustable delay lines. We have shown that the quasi-synchronous primary pumping enables stationary dual-wavelength pulsed lasing in spite of the significant differential group delay (DGD) acquired by the generated fundamental and Stokes pulses during their intracavity round trip under conditions of net normal intracavity dispersion. This DGD can be actively compensated after every round trip by the forced “acceleration” of the fundamental pulses in the rare-earth-doped active fiber provided that the frequency of quasi-synchronous primary pumping is overrated to a proper degree.

We have demonstrated the feasibility and usability of the proposed approach in an experimental trial. We believe that the novel approach may facilitate and advance lidar technologies, laser spectroscopy, and development of mid-infrared coherent pulsed sources.

Supplementary Materials: The following supporting information can be downloaded at: <https://www.mdpi.com/article/10.3390/photonics10010042/s1>, Figure S1: wavelength dependence of the effective refractive index in the P₂O₅-doped fiber used in the study; Figure S2: wide-range spectral scan of the laser radiation accessed via the 5% output coupler following the Yb-doped double-clad active fiber; Figure S3: temporal and spectral traces of the dual-wavelength pulsed lasing obtained at different average pump powers; Figure S4: overlay of temporal traces of the dual-wavelength pulsed lasing obtained at different average pump powers.

Author Contributions: Conceptualization, B.N.; methodology, B.N. and A.I.; software, A.I.; formal analysis, B.N., A.I. and S.S.; investigation, B.N., A.I. and G.V.; resources, A.K., writing—original draft preparation, B.N.; writing—review and editing, A.I., G.V., A.K. and S.S.; visualization, B.N. and A.I.; All authors have read and agreed to the published version of the manuscript.

Funding: Experimental development of the original laser configuration was supported by the Russian Science Foundation (grant No. 17-72-30006-P). Theoretical development of the method (by B.N.) was supported by the Ministry of Science and Higher Education of the Russian Federation (project No. FSUN-2020-0007).

Institutional Review Board Statement: Not applicable.

Informed Consent Statement: Not applicable.

Data Availability Statement: The experimental data presented in this study are available on reasonable request from the corresponding author. The data are not publicly available due to privacy and legal restrictions.

Conflicts of Interest: The authors declare no conflict of interest.

References

1. Zhao, N.; Liu, M.; Liu, H.; Zheng, X.-W.; Ning, Q.-Y.; Luo, A.-P.; Luo, Z.-C.; Xu, W.-C. Dual-wavelength rectangular pulse Yb-doped fiber laser using a microfiber-based graphene saturable absorber. *Opt. Express* **2014**, *22*, 10906–10913. [[CrossRef](#)] [[PubMed](#)]
2. Lau, K.Y.; Bakar, M.H.A.; Muhammad, F.D.; Latif, A.A.; Omar, M.F.; Yusoff, Z.; Mahdi, M.A. Dual-wavelength, mode-locked erbium-doped fiber laser employing a graphene/polymethyl-methacrylate saturable absorber. *Opt. Express* **2018**, *26*, 12790–12800. [[CrossRef](#)] [[PubMed](#)]
3. Liao, R.; Song, Y.; Liu, W.; Shi, H.; Chai, L.; Hu, M. Dual-comb spectroscopy with a single free-running thulium-doped fiber laser. *Opt. Express* **2018**, *26*, 11046–11054. [[CrossRef](#)] [[PubMed](#)]
4. Hussain, S.A. Ultrashort Dual Colour Laser at 1.55 and 1.88 μm by Using a Carbon Nanotube Saturable Absorber. *IEEE Photonics Technol. Lett.* **2019**, *31*, 990–993. [[CrossRef](#)]
5. Li, Y.; Zhao, K.; Cao, B.; Xiao, X.; Yang, C. Carbon nanotube-synchronized dual-color fiber laser for coherent anti-Stokes Raman scattering microscopy. *Opt. Lett.* **2020**, *45*, 3329–3332. [[CrossRef](#)] [[PubMed](#)]
6. Kobtsev, S.; Kukarin, S.; Kokhanovskiy, A. Synchronously pumped picosecond all-fibre Raman laser based on phosphorus-doped silica fibre. *Opt. Express* **2015**, *23*, 18548–18553. [[CrossRef](#)] [[PubMed](#)]
7. Kharenko, D.; Efremov, V.; Evmenova, E.; Babin, S. Generation of Raman dissipative solitons near 1.3 microns in a phosphosilicate-fiber cavity. *Opt. Express* **2018**, *26*, 15084–15089. [[CrossRef](#)] [[PubMed](#)]
8. Kobtsev, S.; Ivanenko, A.; Kokhanovskiy, A.; Gervaziev, M. Raman-converted high-energy double-scale pulses at 1270 nm in P2O5-doped silica fiber. *Opt. Express* **2018**, *26*, 29867–29872. [[CrossRef](#)] [[PubMed](#)]
9. Plotnichenko, V.; Sokolov, V.; Koltashev, V.; Dianov, E. On the structure of phosphosilicate glasses. *J. Non-Cryst. Solids* **2002**, *306*, 209–226. [[CrossRef](#)]
10. Salceda-Delgado, G.; Martinez-Rios, A.; Ilan, B.; Monzon-Hernandez, D. Raman response function and Raman fraction of phosphosilicate fibers. *Opt. Quantum Electron.* **2012**, *44*, 657–671. [[CrossRef](#)]
11. Babin, S.A.; Podivilov, E.V.; Kharenko, D.S.; Bednyakova, A.E.; Fedoruk, M.P.; Kalashnikov, V.L.; Apolonski, A. Multicolour nonlinearly bound chirped dissipative solitons. *Nat. Commun.* **2014**, *5*, 4653. [[CrossRef](#)] [[PubMed](#)]
12. Kharenko, D.; Bednyakova, A.; Podivilov, E.; Fedoruk, M.; Apolonski, A.; Babin, S. Feedback-controlled Raman dissipative solitons in a fiber laser. *Opt. Express* **2015**, *23*, 1857–1862. [[CrossRef](#)] [[PubMed](#)]
13. Chang, S.; Wang, H.; Wang, Z.; Yang, H. Generation of coherent multicolor noise-like pulse complex in Yb-doped fiber laser mode-locked by GIMF-SA. *Opt. Express* **2021**, *29*, 14336–14344. [[CrossRef](#)] [[PubMed](#)]
14. Smirnov, S.; Nyushkov, B.; Ivanenko, A.; Kolker, D.; Kobtsev, S. Shaping of nanosecond pulses in ytterbium fiber lasers by synchronous sine-wave pump modulation. *J. Opt. Soc. Am. B* **2020**, *37*, 3068–3076. [[CrossRef](#)]
15. Nyushkov, B.; Ivanenko, A.; Smirnov, S.; Kobtsev, S. High-energy pulses from all-PM ultra-long Yb-fiber laser mode-locked with quasi-synchronous pumping. *Opt. Fiber Technol.* **2021**, *66*, 102650. [[CrossRef](#)]
16. Bukhman, N.S. On the propagation velocity of a wave packet in an amplifying medium. *Quantum Electron.* **2001**, *31*, 774–780. [[CrossRef](#)]
17. Kharenko, D.S.; Podivilov, E.V.; Apolonski, A.A.; Babin, S.A. 20 nJ 200 fs all-fiber highly chirped dissipative soliton oscillator. *Opt. Lett.* **2012**, *37*, 4104–4106. [[CrossRef](#)] [[PubMed](#)]
18. Wang, J.Z.; Luo, Z.Q.; Cai, Z.P.; Zhou, M.; Ye, C.C.; Xu, H.Y. Theoretical and Experimental Optimization of O-Band Multiwavelength Mixed-Cascaded Phosphosilicate Raman Fiber Lasers. *IEEE Photonics J.* **2011**, *3*, 633–643. [[CrossRef](#)]

Disclaimer/Publisher’s Note: The statements, opinions and data contained in all publications are solely those of the individual author(s) and contributor(s) and not of MDPI and/or the editor(s). MDPI and/or the editor(s) disclaim responsibility for any injury to people or property resulting from any ideas, methods, instructions or products referred to in the content.